International Journal of Engineering Research and Technology. ISSN 0974-3154, Volume 12, Number 12 (2019), pp. 3032-3037

A Mathematical Model of Sediment Transport of the Poti Coastal Zone

Ivane Saghinadze[1], Manoni Kodua[2]

[1]Professor, Akaki Tsereteli State University, Poti Maritime and Transport Faculty, King Tamar str. 59, Kutaisi, 4600 Georgia.

[2]Assistnat Professor, Georgian Technical University, Department of Hydro-engineering Kostava str. 77, Tbilisi, 0171 Georgia.

ORCID: 0000-0002-3186-9062 (Manoni Kodua)

Abstract

The article presents a mathematical model of sediment transport and changes in the topography of the Black Sea seabed in the Poti region. Wave motions, coastal flows, sediment transport and accordingly changes in the topography of the seabed are interconnected. Therefore, in solving the problem of sediment transport, the data of wave motions and their flows are needed. For quantitative and qualitative analysis of sediment transport rate, the equation of mass conservation for sediments is used. By means of Green's equation, the mass conservation equation is transformed and solved by the finite element method. Finite difference schemes are built using Courant functions in considered area. In order to apply approximate equation for temporal term of the equations, instead of the evolutionary problem, we obtain the Cauchy problem. To construct temporal approximations associated with the solution of the obtained equations, Crank-Nicolson schemes are used, that provide the second order of approximation in time. As a result of such transformations, the initial equations of sediment mass conservation will be reduced to a system of algebraic equations, which are solved by the upper relaxation method.

A numerical study was conducted and numerical values of sediment transport rate and seabed depth changes were obtained.

The average annual coastal erosion rate is approximately 7-10 m/year. The shortage of beach-forming material in the south of the port is approximately 200,000 - 250,000 m^3/year.

The obtained results in the given article fully coincide with the results received using observations and measurements conducted by the "Georgian State Hydrographic Service" in 1990-2018.

Keywords: Wave Motion, Coastal Erosion, Sediment, Numerical Model.

I. INTRODUCTION

Environmental forcing that are relevant for most coastal CC impacts studies are water levels, offshore waves, coastal currents, and river flow. Pre-determined water levels are usually specified as boundary conditions in coastal impact models. Commonly used models to simulate ocean waves at regional scale include: WAM [5], SWAN [2], Mike21SW [20], and WaveWatch3 [22]. Widely used models to simulate regional scale coastal currents include: Delft3D [9], MIKE21 FM [12], and NEMO-POA [10]. Land surface models (LSMs) commonly used to simulate river flow include: SiB variants [13], and ISBA [3].

Study of beach lithodynamics due to changes in longshore sediment transport may be readily simulated with one-line models such as LITLINE, UNIBEST-CL, GENESIS and CEM [15, 16, 21].

As beach changes is governed by both longshore and cross-shore sediment transport [6, 14], 2004, Harley et al., 2011), a fully 3D (or at least Quasi 3D) process based coastal area morphodynamic model which resolves the vertically non-uniform structure of cross-shore currents may be used to simulate these phenomena (e.g. Delft3D in 3D mode). However, presently available 3D or Quasi 3D coastal area models mostly concentrate on simulating bed level changes below MWL and do not incorporate the ability to accurately simulate coastline change.

Another approach to simulate beach change is to link a one-line coastline change model with a 2DV coastal profile model. This approach was adopted by Huxley (2011) where a coastline model based on the CERC equation was coupled with Miller and Dean's (2004) cross-shore profile model.

However, the application of the above-mentioned models in order to study the litho-dynamics of the Poti region of the Black Sea due to the complexity of the bottom relief and coastal zone (underwater canyons, port barriers, piers, river run-off, etc.) does not give reliable results.

Black Sea coast of Poti region faces significant impacts from the Rioni River. Since 1939, the serious environmental problems started in Poti after diversion of the main stream of river Rioni at the 7th km to the northeast of Poti. As a result, the flooding of the city had stopped, however the reduction of water consumption in the old channel caused a decrease of the sediments carried away by the river, which leads to coastal washing-out (Fig. 1). In order to solve this problem, in 1959 the water distribution structure was built on the given river, which included a dam-bridge and regulator. Unfortunately, due to the errors made during the design process, given structure unable to implement its protection function [4].

The coastal changes are associated with the movement of waves and flows in the coastal part of the sea.

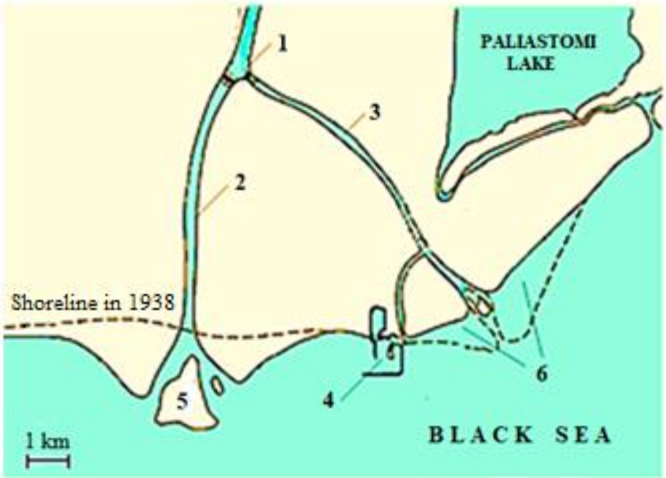

Fig. 1. Master Plan of Poti region: 1 - Water distribution structure on the Rioni River; 2 - new river flow (1939); 3 - old river bed; 4 - city port; 5 - the island formed after the diversion of the stream; 6 - washout area after flow diversion

Sediment transport in the coastal zone of the sea causes changes in the topography of the seabed. For quantitative and qualitative analysis of the sediment transport rate we will use a model that is largely similar to the well-known models [1,7]. The difference lies in the method of finding an approximate solution of the investigated equations.

II. MATHEMATICAL MODEL

As it is known from the mass conservation equation for sediments, the changes in water depth h can be written as follows [7]:

$$\frac{\partial h}{\partial t} = \frac{\partial q_x}{\partial x} + \frac{\partial q_y}{\partial y} \tag{1}$$

where x and y are horizontal coordinates, q_x and q_y - sediment transport rate within the element in direction x and y. Volumetric transport rates (q_x, q_y) expressed in terms of the effective volume of sediment transmitted by the vertical cross section of the element per unit of time.

Horikawa (1988) proposed the following equation for determining the rate of sediment transport:

$$(q_x, q_y) = (q_{cx}, q_{cy}) + (q_{wx}, q_{wy}) \tag{2}$$

here (q_{cx}, q_{cy}) are sediment transport caused by the averaged flows, (q_{wx}, q_{wy}) - sediment transport caused by waves. Sediment transport caused by average flows is determined by the equations:

$$q_{cx} = Q_c U,\ q_y = Q_c V,\ \ Q_c = A_c(\tau_m - \tau_{cr})/\rho g \tag{3}$$

where U and V are averaged flow rates in the direction x and y, A_c - dimensionless ratio of the order of 0,1-1, τ_m - the maximum value of seabed shear stress under the mutual action of waves and flow $\tau_m = \frac{1}{2}\rho f_{cw}\hat{u}_b^2$, $\hat{u}_b^2$ - near-seabed orbital velocity amplitude, f_{cw} - seabed friction ratio, τ_{cr} - critical shear stress of the seabed at the beginning of movement of sediment. If $\tau \le \tau_{cr}$, $Q_c = 0$. Equations (3) are based on the concept of a force model, i.e. sediment volume Q_c is proportional to the combined shear stress.

Wave transport of sediments is caused by asymmetry of the seabed wave velocity and is more complicated because requires consideration of factors such as refraction, diffraction, reflection and collapse of waves, as well as the slope of the seabed. The equations for determining transport rate of sediments caused by wave motion looks like [4]:

$$q_{wx} = F_d Q_w \hat{u}_b \cos\alpha\ , q_{wy} = F_d Q_w \hat{u}_b \sin\alpha\ , \tag{4}$$

$$Q_w = A_w(\tau_m - \tau_{cr})/\rho g$$

where A_w is dimensionless ratio, $\hat{u}_b$ - near-seabed orbital velocity amplitude, α- angle between the direction of wave propagation and the axis x. Dimensionless ratio A_w is equal to:

$$A_w = B_w \frac{w_0}{(1-\lambda_v)s\sqrt{sgd}}\sqrt{\frac{f_w}{2}}, \tag{5}$$

$S = (\rho_s - \rho)/\rho$, τ_m- maximum shear stress due to waves and flows, λ_v- seabed porosity, f_w- wave friction ratio. The value of f_w depends on the amplitude and period, orbital velocity and characteristics of the seabed. For example, if the seabed is formed from sand $d = 0.2$ mm, $w_{w0} = 2.4$Cm/s, $\lambda_v = 0.4$, $s = 1.65$, $B_w = 7$ and $f_w = 0.01 \sim 0.2$, then according to equation (5), the values of A_w vary within the range 0.2~0.9. In calculations, the coefficient A_w is assumed as constant. In the equations (4) F_d is equal to:

$$F_d = \tanh\left(\frac{\Pi_c - \Pi}{\Pi_c}\right), \qquad \Pi = \psi' \frac{h}{L_0} = \frac{\hat{u}_b^2}{sgd}\frac{h}{L_0}, \tag{6}$$

where Π_c is the critical value of Π at zero point (where the transverse sediment transport is 0). The values of Π_c are values of the order of one and specified in the calculation process. The parameter Π value is specified, if ψ' replaced by the Shields parameter $(\psi_m = \tau_m/(\rho_s - \rho)/\rho)gd)$.

Formulas (3, 4) depend on seabed friction (critical shear stress), the values of which must be determined. Critical condition of sediment movement under the waves and flows influence is determined by critical volume of Shields parameter:

$$\psi_c = \tau_{cr}/(\rho_s - \rho)gd \tag{7}$$

According to Watanabe et al., [1986], the value of the critical Shields parameter for fine sand $(d = 0.1 \sim 0.4)$ is equal to 0.11 for coarse sand – 0.06.

In the equations for determining (q_x, q_y) the seabed slope effect was not taken into account. The following equations were introduced to account for the slope of the seabed:

$$q'_x = q_x + \varepsilon_s |q_x| \frac{\partial h}{\partial x}, \quad q'_y = q_y + \varepsilon_s |q_y| \frac{\partial h}{\partial y}\ , \tag{8}$$

and instead of equation (1) we obtain:

$$\frac{\partial h}{\partial t} = \frac{\partial q'_x}{\partial x} + \frac{\partial q'_y}{\partial y}. \tag{9}$$

II.I. Solution algorithm

In equation (9) were introduced notations:

$$A = q_x,\ B = \varepsilon_s |q_x|\ ,\quad C = q_y, \qquad D = \varepsilon_s |y|$$

and were rewritten as:

$$\frac{\partial h}{\partial t} = \frac{\partial}{\partial x}\left(A + B\frac{\partial h}{\partial x}\right) + \frac{\partial}{\partial y}\left(C + D\frac{\partial h}{\partial y}\right) \tag{10}$$

Let's formulate a generalized statement of the problem. If we denote the generalized solution of problem (9) with the function $h \in \widetilde{W}_2^{(1)}$ ($\widetilde{W}_2^{(1)}$ - Sobolev space) the following equation would be satisfied:

$$\iint_S \frac{\partial h}{\partial t}\omega_{i,j} dS = \iint_S \frac{\partial}{\partial x}\left(A + B\frac{\partial h}{\partial x}\right)\omega_{i,j} dS + \iint_S \frac{\partial}{\partial x}\left(C + D\frac{\partial h}{\partial x}\right)\omega_{i,j} dS \tag{11}$$

For any $\omega_{i,j} \in \widetilde{W}_2^{0(1)}$. Here $\widetilde{W}_2^{0(1)}$ is the space of square-integrals functions, together with their first derivatives, equal to zero on the boundary B and taking arbitrary fixed values within the area S [23].

Applying in equation (11) Green's formula we obtain:

$$\iint_S \frac{\partial h}{\partial t}\omega_{i,j} dS = -\iint_S \left(A + B\frac{\partial h}{\partial x}\right)\frac{\partial \omega_{i,j} dS}{\partial x} - \iint_S \left(C + D\frac{\partial h}{\partial y}\right)\frac{\partial \omega_{i,j}}{\partial y} dS. \tag{12}$$

Afterwards, let's proceed to the construction of the approximating scheme. In the S area we construct a grid rectangular area the S_n with a step the $a = \Delta x$ and $b = \Delta y$. Triangulate the area by separating the rectangles of the grid with diagonals of positive direction. The projection-difference scheme will be built as following: to each node of the grid of (x_i, y_j) of S_n area we put in accordance with Courant function $\omega_{i,j}$, which is equal to 1 in this node and equal to 0 in all other nodes of the grid:

$$\omega_{m,n}(x_i, y_j) = \begin{cases} 1, (i,j) = (m,n) \\ 0, (i,j) \neq (m,n) \end{cases}. \tag{13}$$

The functions $\omega_{m,n}(x_i, y_j)$ have a hexagon carrier represented in Fig. 2.

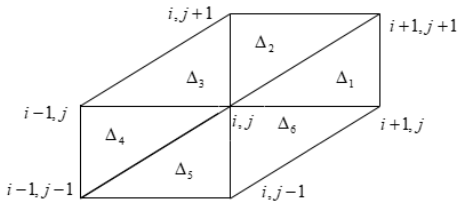

Fig. 2. Finite element

Interpolation functions of $\omega_{i,j}$ are defined as following:

$$(x,y) = \begin{cases} (x_{i+1,j} - x)/a, \dots\dots\dots\dots\dots\dots\dots\ \dots \text{ at}(x,y) \in \Delta_1; \\ (y_{i+1,j} - y)/b, \dots\dots\dots\dots\dots\dots\dots\ \dots \text{at}(x,y) \in \Delta_2; \\ (x - x_{i,j})/a + (y_{i,j+1} - y)/b, \dots\dots \text{ at}(x,y) \in \Delta_3; \\ (x - x_{i-1,j})/a, \dots\dots\dots\dots\dots\dots\dots\ \dots \text{ at}(x,y) \in \Delta_4; \\ (y - y_{i,j-1})/b, \dots\dots\dots\dots\dots\dots\dots\ \dots \text{ at}(x,y) \in \Delta_5; \\ (x_{i+1,j} - x)/a + (y_{i,j+1} - y)/b, \dots \text{ at}(x,y) \in \Delta_6. \end{cases} \tag{14}$$

The values of the derivatives of $\omega_{i,j}$ functions on the base triangles will be constant. They are presented in the Table 1.

Table 1. Derivatives of base functions

Triangles / Functions	Δ_1	Δ_2	Δ_3	Δ_4	Δ_5	Δ_6
$\frac{\partial \omega_{i,j}}{\partial x}$	$-\frac{1}{a}$	0	$\frac{1}{a}$	$\frac{1}{a}$	0	$-\frac{1}{a}$
$\frac{\partial \omega_{i,j}}{\partial y}$	0	$-\frac{1}{b}$	$-\frac{1}{b}$	0	$\frac{1}{b}$	$\frac{1}{b}$

The approximate solution of equation (12) may be presented in the following form:

$$h = \sum_{i,j \in S^n} h_{i,j}(t)\omega_{i,j}(x,y) \tag{15}$$

The function $\omega_{i,j}(x,y)$ is non-zero only in six triangles of the area adjacent to the angle$\omega_{i,j}(x_i, y_j)$. Therefore, the integration in equation (12) was carried out only by combination of these triangles. The function $h_{i,j}(x,y)$ looks like (decomposing into a Taylor series in the neighborhood of point (i,j) and keeping the first two terms):

$$h_{i,j}(x,y) = \begin{cases} h_{i,j} + h_{(i,j)x}(x - x_{i,j}) + h_{(i,j)y}(y - y_{i,j}), - \text{ in } \Delta_1; \\ h_{i,j} + h_{(i,j)x}(x - x_{i,j}) + h_{(i,j)y}(y - y_{i,j}), - \text{in } \Delta_2; \\ h_{i,j} + h_{(i,j)\bar{x}}(x - x_{i,j}) + h_{(i,j)y}(y - y_{i,j}), - \text{in } \Delta_3; \\ h_{i,j} + h_{(i,j)\bar{x}}(x - x_{i,j}) + h_{(i,j)\bar{y}}(y - y_{i,j}), - \text{in } \Delta_4; \\ h_{i,j} + h_{(i,j)\bar{x}}(x - x_{i,j}) + h_{(i,j)\bar{y}}(y - y_{i,j}), - \text{in } \Delta_5; \\ h_{i,j} + h_{(i,j)x}(x - x_{i,j}) + h_{(i,j)\bar{y}}(y - y_{i,j}), - \text{in } \Delta_6. \end{cases} \tag{16}$$

Derivatives $h_{i,j}$ on the triangles of area S_n are shown in the Table 2.

Table 2. Derivative functions $h_{i,j}$

Triangles / Functions	Δ_1	Δ_2	Δ_3	Δ_4	Δ_5	Δ_6
$\frac{\partial h_{i,j}}{\partial x}$	$\frac{h_{i+1,j} - h_{i,j}}{a}$	$\frac{h_{i+1,j+1} - h_{i,j+1}}{a}$	$\frac{h_{i,j} - h_{i-1,j}}{a}$	$\frac{h_{i,j} - h_{i-1,j}}{a}$	$\frac{h_{i,j-1} - h_{i-1,j-1}}{a}$	$\frac{h_{i+1,j} - h_{i,j}}{a}$
$\frac{\partial h_{i,j}}{\partial y}$	$\frac{h_{i+1,j+1} - h_{i,j+1}}{b}$	$\frac{h_{i,j+1} - h_{i,j}}{b}$	$\frac{h_{i,j+1} - h_{i,j}}{b}$	$\frac{h_{i-1,j-1} - h_{i-1,j}}{b}$	$\frac{h_{i,j} - h_{i,j-1}}{b}$	$\frac{h_{i,j} - h_{i,j-1}}{b}$

To find coefficients of $h_{i,j}(t)$ using a quadrature formula to calculate the evolutionary term, equation (12) was written as:

$$\left(\iint\limits_S \frac{\partial h}{\partial t}\omega_{i,j}dS\right)\frac{dh_{i,j}}{dt}+\iint\limits_S\left(A+B\frac{\partial h}{\partial x}\right)\frac{\partial \omega_{i,j}}{\partial x}dS + \iint\limits_S\left(C+D\frac{\partial h}{\partial y}\right)\frac{\partial \omega_{i,j}}{\partial y}dS=0. \quad (17)$$

Substituting into (17) the expression (15), we get:

$$\theta\frac{\partial \vec{h}}{\partial t}+E\vec{h}=0,\ \vec{h}(0)=\vec{h}_0,\ \theta=\Delta xy=ab \quad (18)$$

It should be noted that approximate equations were used for approximations of the temporal term:

$$\left(\dot{\vec{h}},\omega_{i,j}\right)=\theta\dot{\vec{h}}_{\ i,j} \quad (19)$$

This allows us to consider the Cauchy problem instead of general evolutionary problem with the averaging operator at a temporal term and allows to simplify calculations. As it is known, the approximation properties do not change [11].

In eq.18, the coefficients are equal to:

$$E_1=\frac{b}{6a}\left(4B_{i,j}+2B_{i+1,j}+B_{i+1,j+1}+B_{i,j+1}+2B_{i-1,j}+B_{i,j-1}\right)$$
$$+\frac{a}{6b}\left(D_{i+1,j+1}+2D_{i,j+1}+D_{i-1,j}+D_{i-1,j-1}+2D_{i,j-1}+D_{i+1,j}\right);$$
$$E_2=\frac{b}{6a}\left(2B_{i,j}+2B_{i+1,j}+B_{i+1,j+1}+B_{i,j-1}\right)$$
$$E_3=\frac{a}{6b}\left(2D_{i,j}+D_{i+1,j+1}+2D_{i,j}+D_{i-1,j}\right)$$
$$E_4=\frac{b}{6a}\left(2B_{i,j}+B_{i,j+1}+2B_{i-1,j}+B_{i-1,j-1}\right) \quad (20)$$
$$E_5=\frac{a}{6b}\left(2D_{i,j}+D_{i-1,j-1}+2D_{i,j-1}+D_{i+1,j}\right)$$
$$F=\frac{b}{6}\left(A_{i+1,j}+A_{i+1,j+1}-A_{i,j+1}-A_{i-1,j}-A_{i-1,j-1}+A_{i,j-1}\right)$$
$$+\frac{a}{6}\left(C_{i+1,j+1}+2C_{i,j+1}-C_{i-1,j}-C_{i-1,j-1}-2C_{i,j-1}-C_{i+1,j}\right).$$

To construct temporal approximations associated with solving equations (20), Crank-Nicholson schemes can be used, which provide a second order of approximation of time [11]. We approximate problem (20) as follows:

$$h_{i,j}^{m+1}\left[\frac{ab}{\Delta t}+\frac{E_1}{2}\right]-h_{i+1,j}^{m+1}\frac{E_2}{2}-h_{i,j+1}^{m+1}\frac{E_3}{2}-h_{i-1,j}^{m+1}\frac{E_4}{2}-h_{i,j-1}^{m+1}\frac{E_5}{2}=$$
$$=h_{i,j}^{m}\left[\frac{ab}{\Delta t}-\frac{E_1}{2}\right]+h_{i+1,j}^{m}\frac{E_2}{2}+h_{i,j+1}^{m}\frac{E_3}{2}+h_{i-1,j}^{m}\frac{E_4}{2}+h_{i,j-1}^{m}\frac{E_5}{2}+F. \quad (21)$$

Eq.(21) under the corresponding boundary, the conditions and initial data are effectively solved by the upper block relaxation method.

Solving the problem of changing the topography of the bottom requires wave and coastal current data, that were calculated in [7]. According to the equations (8) determining the velocity of sediment transport we get:

$$q_x=F_dQ_w\hat{u}_b\cos\alpha+Q_cU;\ \ q_y=F_dQ_w\hat{u}_b\sin\alpha+Q_cU \quad (22)$$

where

$$Q_c=A_c(\tau_m-\tau_{cr})/\rho g,\ Q_w=A_w(\tau_m-\tau_{cr})/\rho g,$$
$$F_d=\tanh\left(k_{md}\frac{\Pi_c-\Pi}{\Pi_c}\right);$$

U and V are averaged flow rates; $\hat{u}_b$ near-seabed orbital velocity amplitude; α– wave propagation angle relative to the x-axis; A_w–coefficient, which values are in the range of $0.2-0.9$; A_c– dimensionless coefficient of the order, about $0.1-1$; τ_m – the maximum seabed shear stress is equal to $\tau_m=\frac{1}{2}\rho f_{cw}\hat{u}_b^2$; f_{cw}– coefficient of seabed friction together with the waves and flows and is equal to $f_{cw}=0.07-0.1$; –critical seabed shear stress to start sediment movement:

in the surf zone $\tau_{cr}=0$, out of the surf zone

$$\tau_{cr}=\psi_c\,(\rho_s-\rho)grad\tanh^2(k_cx_b/X_b) \quad (23)$$

ψ_c is the critical value of the Shields parameter which is equal to:

$$\psi_c=\begin{cases}0{,}11 \text{ \_ if } d/\delta_L<1/6.5\\ 0{,}06 \text{ \_ if } d/\delta_L>1/4\end{cases}, \quad (24)$$

d is characteristic diameter of beach-forming sediment (sand); $\delta_L=\sqrt{vT/\pi}$ – the thickness of the near-seabed layer; v– kinematic viscosity and $v=1.306\cdot10^{-6}m^2/S$, at $t=10°$;

Π calculated by the eq.6. Π_c is is a critical value of Π at the zero point (where transverse sediment transport is zero). Values of Π_c the order of unity are determined by the calibration calculations ($S=(\rho_s-\rho)/\rho$).

The five-point eq.20

$$-h_{i-1,j}^{m+1}E_4+h_{i,j}^{m+1}\left[\frac{2ab}{\Delta t}+E_1\right]-h_{i+1,j}^{m+1}E_2=h_{i,j+1}^{m+1}E_3-h_{i,j-1}^{m+1}E_5+$$
$$+h_{i,j}^{m}\left[\frac{2ab}{\Delta t}-E_1\right]+h_{i+1,j}^{m}E_2+h_{i,j+1}^{m}E_3+h_{i-1,j}^{m}E_4+h_{i,j-1}^{m}E_5+2F. \quad (25)$$

II.II. Computing Experiments

Equation (25) is solved by upper relaxation method [11]. The solution requires to determine the size of the computation area, the grid interval and time increments that depends on the modelling area. Topographic maps of the investigated area are used as an initial condition. For the purpose of calibrating the model or adjusting various coefficients, bathymetric observations at various stages of the past are very significant. The offshore border was taken at such a distance from the coast, where it is known in advance that changes in the topography of the seabed will be negligible. For the Poti coast such a border is at a depth of 10-15 m [19].

The existing model of sediment transport and seabed topography changes includes seven coefficientsA_c,,A_w, τ_{cr}, k_c, Π_c, k_d, ε_s. The variables for different areas of the coastal zone are different and determined by computational experiments. Coefficients A_c and A_w in transport of sediments equations are taken respectively 0.1 and 1. The values of A_c and A_w should be calibrated by comparing the calculated results of the coastal changes with measurements in the areas, where the solution is known in advance. The critical share stress τ_{cr} is determined from equations (23)-(24), where k_c is taken on the order of unity. The value of the coefficient Π_c is assumed to be 0,16 and $k_d = 2$, they should be further clarified by calibration calculations. Calibration calculations are also required for the coefficient ε_s, which controls the effect of slope of the seabed. This coefficient has the additional effect of suppressing not only physical, but also numerical computational disorders. Initial values of are taken in the range 1–10.

While solving equation (25), we consider the coastal area, which is located at the southern mole of the port of Poti. The location of the grid is shown in Fig.3. The x-axis is perpendicular to the shore and the y-axis is parallel. The intervals of the grid partition are equal to $a = \Delta x = 5m$, $b = \Delta y = 50m$. On the x-axis is 141 points, and on the y-axis - 13, total of 1833 points.

In the first step, the initial topography of the coast and the geometry of the structures are given as input parameters. Then, the coastal wave field for the prescribed conditions of the initial wave is calculated. The calculated wave field is used to estimate the spatial distribution of radiation and near-seabed orbital velocities. The calculation of coastal flows follows the wave field [18]. Coastal wave and current fields are used in a sub-model of sediment transport and coastal topography changes.

Fig. 3. Scheme of the modelling area

Let us consider an example when sea waves are caused by western waves with a height of 1 m, a period of 4 seconds and a length of 25 m. The diameter of the sand grains is taken in the range of 0.2 - 0.3 mm.

The results of the numerical solution are shown in Fig. 4-6. Model time is 180 minutes; time step is 0.001 seconds. When calculating the average elevation of sea level, the initial value was 0.1 m, which corresponds to real conditions. Changes in sediment transport rates in the transverse direction to the coast and along the coast are shown in Fig. 4-6.

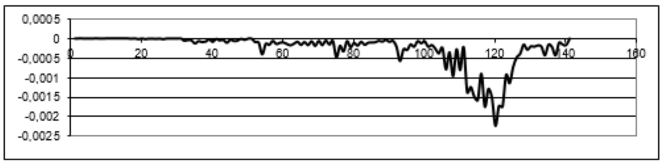

Fig. 4. Sediment transport rates q_x[m^2/s], at i=1-141, j=5

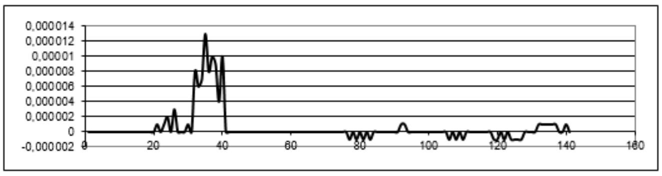

Fig. 5. Sediment transport rates q_y[m^2/s] at i=1-141, j=5

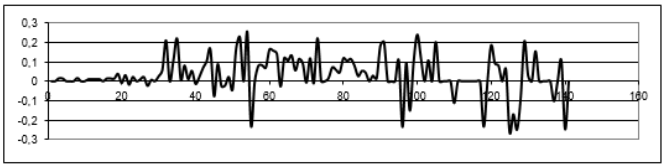

Fig. 6. Changing the seabed topography Δh[m] at i=1-141, j=5

III. CONCLUSION

Wave motion, coastal flows and changes in coastal topography are interrelated. To include this interaction in the model, an additional iteration of the wave calculations, the flow and the change in the topography of the bottom with a rather short time interval is required. However, the computation time for the sub-models is not enough to allow a multiple number of nested iterations. Practically, time interval for performing iterations should be determined by considering the expected accuracy of the solution, as well as the required calculation time.

From Fig. 4 it is clear that, when the sediment transport velocity q_x is disturbed at water depths of 10-15 m, it is almost zero. They become significant only at depths of 8-10 meters at $i = 50 - 141$; $j = 1 - 13$. In the case of western waves, the sediment transport rate q_x is directed against the x-axis, their maximum values vary in the range of 0.0015-0.0022 m^2/s. The sediment transport rate along y-axis in this case is insignificant. It manifests itself at points $i = 20 - 40$; $j = 1 - 12$, which is caused by the flow of water in the direction of the y-axis (Fig. 5). The maximum values of sediment transport rates $q_y$are in the range of 0.00001-0.000013 m^2/s [4].

Calculation results of the changes in the topography of the seabed in the coastal zone are presented in the Fig. 6. A negative value of Δh corresponds to coastal erosion and a positive value corresponds to accumulation and Δh varies from 0,29 to 0,26 m. In the surf zone at $i = 120 - 141$; $j = 1 - 9$, costal erosion is observed. After calibration of the model, additional numerical calculations were carried out for Poti on the Black Sea coast in the areas north and south of the runoff of the "city channel" on the old river-bed of Rioni River (Fig. 1). As a result, we get:

- From the place of runoff of the "city canal" of the old riverbed of the Rioni River (Fig. 1; 3) to the protective breakwater (Fig. 1; 4), the average annual costal erosion rate is approximately 7–8 m/year;
- South of the runoff of the "city canal" of the old riverbed of the Rioni River (Figs. 1, 3), the average annual erosion rate is approximately 8–10 m/year;

- The shortage of beach-forming material in this area of the coast is approximately 200,000 - 250,000 m^3/year.

IV. ACKNOWLEDGEMENTS

This work was supported by Shota Rustaveli National Science Foundation of Georgia (SRNSFG) [grant number YS17_65].

REFERENCES

[1] Bowden K. F., 1983. Physical Oceanography of Coastal Waters. New York, Ellis Harwood Limited, 302 p.

[2] Booij N., Ris R.C., Holthuijsen L.H. A third generation wave model for coastal regions. Part 1: model description and validation. J. Geophys. Res., 104 (C4) (1999), pp. 7649-7666.

[3] Etchevers P., Colaz C., Habets F. Simulation of the water budget and the rivers flows of the Rhone basin from 1981 to 1994. J. Hydrol., 244 (2001), pp. 60-85.

[4] Gagoshidze Sh., Kodua M., Saghinadze I., and Kadaria I. 2017. River hydro construction and geomorphological processes in the Black Sea coast of Georgia. 1st ed. Technical University, Tbilisi, 192 p. (in Georgian).

[5] Hasselmann S., Hasselmann K., Janssen P.A.E.M.E., Bauer E., Komen G.J., Bertotti L., Lionello P., Guillaume A., Cardone V.C., Greenwood J.A., et al. The WAM model - A third generation ocean wave prediction model. J. Phys. Oceanogr., 18 (1988), pp. 1775-1810.

[6] Harley M.D., Turner I., Short A.D., Ranasinghe R. A re-evaluation of coastal embayment rotation in SE Australia: the dominance of cross-shore versus alongshore sediment transport processes. J. Geophys. Res. Earth Surf. (2011).

[7] Horikawa K. 1988. Nearshore Dynamics and Coastal Processes. University of Tokyo Press. 522 p.

[8] Huxley C.D. Quantification of the physical impacts of climate change on beach shoreline response. (M. Phil Thesis). The University of Queensland, Brisbane (2011), p. 141.

[9] Lesser G., Roelvink J.A., Van Kester J.A.T.M., Stelling G.S. Development and validation of a three-dimensional morphological model. Coast Eng., 51 (2004), pp. 883-915.

[10] Madec G. NEMO ocean engine. Note du Pole de modélisation, Institute Pierre-Simon Laplace (IPSL). France, 27 (2008), pp. 1288-1619.

[11] Marchuk G., and Sarkisyan A. 1988. Mathematical Modeling of Ocean Circulation. Moscow, "Nauka". 304 p. (in Russian).

[12] MIKE 21 & MIKE 3 Flow Model FM Hydrodynamic and Transport Module Scientific Documentation. DHI Group, Horshølm (2005).

[13] Mocko D.M., Sud Y.C. Refinements to SSiB with an emphasis on snow-physics: Evaluation and validation using GSWP and Valdai data Earth Interact., 5 (2001).

[14] Ranasinghe R., McLoughlin R., Short A., Symonds G. The Southern Oscillation Index, Wave Climate, and Beach Rotation. Mar. Geol., 204 (2004), pp. 273-287.

[15] Ratliff K.M., Murray A.B. Modes and emergent time scales of embayed beach dynamics. Geophys. Res. Lett., 41 (2014), pp. 7270-7275.

[16] Ruggiero P., Buijsman M., Kaminsky G.M., Gelfenbau m G. Modeling the effects of wave climate and sediment supply variability on large-scale shoreline change. Mar. Geol., 273 (2010), pp. 127-140.

[17] Saghinadze I., and Arkania Z. 2004. Mathematical model of wave motions in the Surf zone of the Black Sea in the Poti region. Journal of Intelligence. No 2 (19) pp. 42-44(in Georgian).

[18] Saghinadze I. 2013. Calculation of the coastal currents of the Black Sea in the area of Poti. Journal of Georgian Engineering News, No 2 (66) p. 101-104 (in Georgian).

[19] Saghinadze I., Pkhakadze M. The numerical calculation of hydrological processes in the coastal zone of the Black Sea region in the city of Poti. Paper presented at European Geosciences Union to be held in Vienna, Austria, April 2016. Published abstract.

[20] Serensen O. R., Kofoed-Hansen H., Rugbjerg M., Serenson L.S.A third-generation spectral wave model using an unstructured finite volume technique. Proceedings of the 29th International conference on coastal engineering, Lisbon, Portugal (2004), pp. 894-906.

[21] Slott J.M., Murray B., Ashton D., Crowley T. J. Coastline response to changing storm patterns. Geophys. Res. Lett., 33 (2006), p. L01602.

[22] Tolman, H. L., 2009b: User manual and system documentation of WAVEWATCH III TM version 3.14. Tech. Note 276, NOAA/NWS/NCEP/MMAB, 194 pp..

[23] Tvalchrelidze A., Saghinadze I, and Arkania Z. 2000. Finite Element Model of the Dynamics of Waves in the Coastal Zone of the Sea. Journal of Georgian Engineering News, No 3. pp. 65-67)in Georgian).

[24] Watanabe A., K. Maruyama, T. Shimizu, and T. Sakakiyama. 1986: Numerical prediction model of three-dimensional beach deformation around a structure. Journal of Coastal Engineering in Japan, No 1 (29) pp. 179-194.